International Journal of Thermophysics, Vol. 12, No. 2, 1991

The Critical Thermal-Conductivity Enhancement Along the Critical Isochore

B. Le Neindre,[1] Y. Garrabos,[1] and R. Tufeu[1]

Received April 16, 1990

We report experimental measurements of the critical thermal-conductivity enhancement along the critical isochore for a number of fluids. The data are analyzed in terms of a corresponding-states treatment which can be used as a predictive method to calculate the thermal-conductivity enhancement along the critical isochore for any fluid. The quantities which are needed are the coordinates of the critical point, the slope of the critical isochore, and the viscosity along the critical isochore.

KEY WORDS: corresponding states; critical phenomena; thermal conductivity.

1. INTRODUCTION

In our laboratory, we have used the coaxial cylinder method to measure the thermal conductivity of several fluids over wide temperature and pressure ranges including the critical region [1]. In the critical region, these experiments are always hampered by specific difficulties, which explain why very few thermal-conductivity data have been reported in that range. The difficulties are related to the experimental conditions: for instance, the critical pressures and temperatures can be relatively high (H_2O and D_2O). Above all, convection must be minimized in order to obtain reliable data; this can be achieved with small temperature gradients and small characteristic lengths of the sample, which are incompatible with accurate measurements. As experiments are not easy to perform, the development of any correlation which can be used as a predictive method for the critical enhancement of the thermal conductivity with a reasonable accuracy will be useful.

[1] LIMHP—CNRS, Centre Universitaire Paris-Nord, Avenue J.B. Clément, 93430 Villetaneuse, France.

0195-928X/91/0300-0307$06.50/0

2. EXPERIMENTAL THERMAL-CONDUCTIVITY DATA

The thermal conductivity was measured with a concentric-cylinder apparatus made of silver and set up in a vertical position. A full description of the apparatus and the various corrections are reported in refs. 2–4. The experimental apparatus was identical for all the fluids investigated. The only procedural difference was in the gap between the cylinders, which could be varied from 0.2 to 0.4 mm. The convective heat flow is estimated from the Rayleigh number:

$$\mathrm{Ra} = G_R P_R = \frac{g\alpha_p \rho^2 c_p e^3 \Delta T}{\eta\lambda} \tag{1}$$

where

G_R = Grashof number

P_R = Prandtl number

g = gravitational constant

ρ = density

$\alpha_p = -(1/\rho)(\partial\rho/\partial T)$ = expansion coefficient

c_p = specific heat at constant pressure

e = thickness of the gas layer

ΔT = temperature difference between the cylinders

λ = thermal conductivity coefficient

η = viscosity coefficient

The Rayleigh number is strongly dependent on the thickness of the layer e. Near the critical point, the smallest gap, 0.2 mm, was used. The temperature of the sample was measured with a 0.02°C accuracy and the pressure with a 0.05% accuracy. For each experimental point the density was calculated. However, in the critical region the calculated densities become inaccurate.

The thermal-conductivity data have to be corrected for heat transferred by convection, radiation, and parasitic heat flows. These corrections depend on the gas under study and on the covered temperature range. The critical thermal-conductivity enhancement is perturbed only by the convective heat transfer, as the two other corrections are also present and are similar far away from the critical point. The convective flow is assumed to

be laminar, and we have estimated the associated heat flow Q_c from the relation [2]

$$Q_c = \mathrm{Ra}\,\frac{2\pi r}{720}\,\lambda\,\Delta T \tag{2}$$

where r is the mean radius of the annular field layer, which is equal to the sum of the radius of the internal cylinder plus half of the thickness ($e/2$) of the fluid layer. When measurements are made along the isotherm closest to the critical temperature, around $T_c + 3$ K, the temperature difference between the two cylinders is very small and of the order of 0.3 K. The Rayleigh number is always less than 10,000 and the ratio of the convective to the conductive heat transfer is less than 3%. The accuracy of the thermal-conductivity measurements is of the order of 2%, which leads to an uncertainty in the critical enhancement of at least 4%.

Measurements were performed along quasi-isotherms at increasing and decreasing pressures. The density change of the gas (argon) used to compress the sample modifies the heat transfer from the cell to the high-pressure vessel, and for each run the temperature of the cell is slightly different.

To describe the behavior of the thermal conductivity $\lambda(T, \rho)$ as a function of the temperature T and the density ρ in the critical region, it is assumed that it can be separated into two additive parts: a background term λ_B and a critical term $\Delta\lambda_c$ [5]. The background term is the sum of the thermal conductivity λ_0 at zero density and the excess thermal conductivity λ_1, which is, to a good approximation, independent of the temperature. Experimental data of the zero-density contribution and the temperature-independent excess function were fitted by polynomials and the value of the background term at the critical density $\lambda_B(T_c, \rho_c)$ reported in Table XII was directly obtained from these correlations. The critical enhancement at the critical density was obtained from a plot of the isothermal thermal-conductivity data as a function of density. In Tables I–XI we present the experimental critical enhancements of the thermal conductivity $\Delta\lambda_c = \lambda(T, \rho_c) - \lambda_B$, where $\lambda_B = \lambda_0(T) + \lambda_1(\rho_c)$, at the critical density ρ_c, as a function of the temperature. Some of these data have already been published for the following gases: ethane [6], propane [7], *n*-butane [8], isobutane [9], carbon dioxide [10], steam [11], heavy water [12], ammonia [13], and sulfur hexafluoride [14]. The measurements on ethylene and *n*-pentane will be published later.

Table I. Thermal-Conductivity Enhancement of Ethane Along Its Critical Isochore

T (K)	$\Delta\lambda_c$ exp ($W \cdot m^{-1} \cdot K^{-1}$)	$\Delta\lambda_c$ cal ($W \cdot m^{-1} \cdot K^{-1}$)	Deviation (%)
308.75	0.0416	0.0436	−4.8
311.32	0.0288	0.0301	−4.5
315.15	0.0211	0.0216	−2.4
323.15	0.0147	0.0145	1.4
335.29	0.0097	0.0102	−5.2

Table II. Thermal-Conductivity Enhancement of Ethylene Along Its Critical Isochore

T (K)	$\Delta\lambda_c$ exp ($W \cdot m^{-1} \cdot K^{-1}$)	$\Delta\lambda_c$ cal ($W \cdot m^{-1} \cdot K^{-1}$)	Deviation (%)
284.34	0.0587	0.0623	−6.1
284.97	0.0547	0.0521	4.8
285.12	0.0521	0.0501	3.8
288.17	0.0276	0.0307	−11.2
294.62	0.0180	0.0186	−3.3
301.41	0.0162	0.0138	14.8

Table III. Thermal-Conductivity Enhancement of Propane Along Its Critical Isochore

T (K)	$\Delta\lambda_c$ exp ($W \cdot m^{-1} \cdot K^{-1}$)	$\Delta\lambda_c$ cal ($W \cdot m^{-1} \cdot K^{-1}$)	Deviation (%)
371.95	0.059	0.0538	8.8
372.15	0.055	0.0508	7.6
372.85	0.044	0.0427	3.0
373.15	0.040	0.0401	−0.2
373.65	0.037	0.0365	1.4
373.80	0.034	0.0357	−5.0
374.15	0.035	0.0338	3.4
375.70	0.027	0.0276	−2.2
376.05	0.030	0.0265	11.7
379.90	0.020	0.0244	−22.0
381.95	0.017	0.0170	0
382.10	0.018	0.0169	6.1
388.00	0.013	0.0130	0
432.60	0.005	0.0055	−10

Table IV. Thermal-Conductivity Enhancement of *n*-Butane Along Its Critical Isochore

T (K)	$\Delta\lambda_c$ exp ($W \cdot m^{-1} \cdot K^{-1}$)	$\Delta\lambda_c$ cal ($W \cdot m^{-1} \cdot K^{-1}$)	Deviation (%)
427.4	0.055	0.0535	2.7
428.8	0.040	0.0389	2.8
431.4	0.028	0.0272	2.9
436.0	0.019	0.0188	1.1
454.2	0.010	0.0097	3.0
480.0	0.006	0.0062	−3.3
518.4	0.004	0.0042	−5

Table V. Thermal-Conductivity Enhancement of Isobutane Along Its Critical Isochore

T (K)	$\Delta\lambda_c$ exp ($W \cdot m^{-1} \cdot K^{-1}$)	$\Delta\lambda_c$ cal ($W \cdot m^{-1} \cdot K^{-1}$)	Deviation (%)
410.23	0.042	0.0419	0.2
412.41	0.030	0.0273	9
416.59	0.020	0.0178	11
417.73	0.019	0.0164	13.7
426.12	0.012	0.0108	10
448.40	0.008	0.0063	21
478.18	0.005	0.0043	14
505.07	0.004	0.0034	15

Table VI. Thermal-Conductivity Enhancement of *n*-Pentane Along Its Critical Isochore

T (K)	$\Delta\lambda_c$ exp ($W \cdot m^{-1} \cdot K^{-1}$)	$\Delta\lambda_c$ cal ($W \cdot m^{-1} \cdot K^{-1}$)	Deviation (%)
471.8	0.0417	0.0420	−0.7
473.5	0.0307	0.0286	6.8
473.8	0.0287	0.0272	5.2
474.9	0.0277	0.0237	14.4
478.85	0.0179	0.0161	10.1
497.2	0.006	0.0078	−30
576.0	0.002	0.0030	−50

Table VII. Thermal-Conductivity Enhancement of CO_2 Along Its Critical Isochore

T (K)	$\Delta\lambda_c$ exp ($W \cdot m^{-1} \cdot K^{-1}$)	$\Delta\lambda_c$ cal ($W \cdot m^{-1} \cdot K^{-1}$)	Deviation (%)
326.15	0.0152	0.0158	−3.9

Table VIII. Thermal-Conductivity Enhancement of H_2O Along Its Critical Isochore

T (K)	$\Delta\lambda_c$ exp ($W \cdot m^{-1} \cdot K^{-1}$)	$\Delta\lambda_c$ cal ($W \cdot m^{-1} \cdot K^{-1}$)	Deviation (%)
625.30	0.2602	0.2676	−2.8
655.04	0.2149	0.2024	5.8
659.17	0.1696	0.1532	9.7
665.61	0.1285	0.1149	10.6
674.04	0.1000	0.0891	10.9
708.17	0.0576	0.0500	13.2
739.77	0.0430	0.0370	14.0
785.07	0.0261	0.0269	−3.1

Table IX. Thermal-Conductivity Enhancement of D_2O Along Its Critical Isochore

T (K)	$\Delta\lambda_c$ exp ($W \cdot m^{-1} \cdot K^{-1}$)	$\Delta\lambda_c$ cal ($W \cdot m^{-1} \cdot K^{-1}$)	Deviation (%)
650.25	0.2111	0.2204	−4.4
654.49	0.1636	0.1563	4.5
658.32	0.1257	0.1267	−0.8
665.77	0.1009	0.0950	5.8
668.79	0.0897	0.0869	3.1
683.56	0.0664	0.0620	6.6
725.54	0.0375	0.0357	4.8
782.02	0.0180	0.0230	−28
784.39	0.0170	0.0226	−33
784.59	0.0200	0.0226	−13

Table X. Thermal-Conductivity Enhancement of NH_3 Along Its Critical Isochore

T (K)	$\Delta\lambda_c$ exp ($W \cdot m^{-1} \cdot K^{-1}$)	$\Delta\lambda_c$ cal ($W \cdot m^{-1} \cdot K^{-1}$)	Deviation (%)
407.85	0.197	0.195	1.0
408.85	0.173	0.156	9.8
409.42	0.143	0.141	1.4
411.50	0.109	0.107	1.8
415.30	0.090	0.077	14.4
417.40	0.084	0.068	19.0
474.10	0.009	0.020	−122

Table XI. Thermal-Conductivity Enhancement of SF_6 Along the Critical Isochore

T (K)	$\Delta\lambda_c$ exp ($W \cdot m^{-1} \cdot K^{-1}$)	$\Delta\lambda_c$ cal ($W \cdot m^{-1} \cdot K^{-1}$)	Deviation (%)
321.69	0.0167	0.0198	−18.6
322.69	0.0148	0.0164	−10.8
325.69	0.0101	0.0113	−11.9
329.49	0.0080	0.0085	−6.3
341.09	0.0037	0.0052	−40.5
350.09	0.0023	0.0041	−105
411.19	0.0010	0.0019	−90

3. REDUCTION OF THE THERMAL-CONDUCTIVITY ENHANCEMENT

A solution of the mode-coupling equations for the dynamics of critical fluctuations, which includes the crossover from the singular behavior of the transport properties of dense gases asymptotically close to the critical point to the regular behavior of these properties far away from the critical point, was developed by Olchowy and Sengers [15, 16]. Their model takes into account the behavior of the thermal conductivity not only along the critical isochore but in the entire density range. They have made a comparison with thermal conductivity data for carbon dioxide, ethane, and methane. For their simplified model [16], which contains only one fluid-dependent parameter in addition to accurate information about the thermodynamic properties and background properties, the maximum average root-mean-square deviation (σ) of the data was found for ethane to be $\sigma = 3.5\%$. For the other substances σ is lower.

The mode–mode coupling theory predicts that the critical thermal conductivity of a gas can be asymptotically written as

$$\Delta\lambda_c = A \frac{k_B T}{6\pi\eta\xi} \rho c_p^c \tag{3}$$

where k_B is the Boltzmann constant, η is the shear viscosity, and ξ is the long-range correlation length. The critical part of the specific heat at constant pressure c_p^c is calculated by

$$c_p^c = c_p - c_v = (T/\rho)(\partial P/\partial T)_\rho^2 K_T \tag{4}$$

where K_T is the isothermal compressibility. A is a universal constant, the theoretical value of which is close to 1 for $t \to 0$, [6, 7, 11, 13], where $t = (T - T_c)/T_c$ is the reduced temperature difference and T_c is the critical temperature.

Along the critical isochore, Eq. (3) can be written as

$$R_c = \frac{\Delta\lambda_c \eta}{k_B [T(\partial P/\partial T)_{\rho_c}]^2} = \frac{A}{6\pi} \frac{K_T}{\xi} \tag{5}$$

where only static divergent properties appear on the right. A recent analysis of these divergent quantities in the critical region carried out by one of us [17] has shown that the reduced compressibilities K_T^* given by

$$K_T^* = K_T P_c Z_c \tag{6}$$

lie asymptotically on a single curve for a number of fluids when they are plotted as a function of the scaled reduced temperature difference $\tau = Y_c(T/T_c - 1)$ along the critical isochore. In Eq. (6), P_c is the critical pressure and Z_c is the critical compressibility factor: $Z_c = P_c m/k_B T_c \rho_c$, where m is the molecular mass. Y_c is defined by

$$Y_c = \left\{ \left[\frac{\partial P(\rho_c, T_c)}{\partial T} \right]_\rho \frac{T_c}{P_c} \right\} - 1 \tag{7}$$

This result assumes also that the reduced correlation length along ρ_c, $\xi^* = \xi/a$, where $a = (k_B T_c/P_c)^{1/3}$ is a single function of τ for $\tau \to 0$.

Consequently,

$$R_c^* = R_c P_c Z_c a = \frac{\Delta\lambda_c \eta}{k_B [T(\partial P/\partial T)_{\rho_c}]^2} P_c Z_c a = \frac{A}{6\pi} \frac{K_T^*}{\xi^*} \tag{8}$$

should be a single function of τ in the asymptotic region.

The previous discussion is restricted to the asymptotic critical temperature range. However in Ref. 17, we have verified that the reduced isothermal compressibility K_T^* is universal in a larger temperature range, in particular, the temperature range which is covered by these experiments. The plot of the experimental isothermal compressibility data reduced by the parameters indicated in Ref. 17 falls on a single curve up to the temperature range $\tau \simeq 1$. If the same is true for the reduced correlation length (but in that case experimental data are not available), Eq. (8) shows that R_c^* falls on a single curve (A being treated as an effective constant).

4. DATA ANALYSIS

We notice that the divergence of the viscosity is small at the approach of the critical point and takes place essentially in a temperature range from T_c to $T_c + 1$ K. As the temperature range of this study is larger than $T_c + 2$ K, we have not taken into account the divergence of the viscosity. Then the viscosity can be estimated from the background viscosity η_B, which is the sum of two terms:

$$\eta_B = \eta_0 + \eta_1 \tag{9}$$

where η_0 is the viscosity at zero density, which varies only with the temperature, and η_1 is the excess of viscosity, which can be considered, in first approximation, only density dependent. Then along the critical isochore the variation of the viscosity with respect to the temperature will be the same as at atmospheric pressure. The viscosities used in Eq. (8) were taken from different sources but mainly from Ref. 18. In these tables, the viscosities are expressed as a function of temperature and pressure. The zero-density contribution (η_0) to the background viscosity was obtained by fitting the data at atmospheric pressure by polynomial in terms of temperature. For each fluid an equation of state was used to calculate the density and the temperature-independent excess function of the viscosity (η_1) was fitted by a polynomial in terms of density [19].

In Fig. 1 we have plotted R_c^* for a number of fluids in the scaled reduced-temperature range, $0.03 < \tau < 3$. Within the experimental uncertainties, the experimental data lie on a single curve. The error in $\Delta\lambda_c$ is the sum of two terms: the error in the experimental thermal-conductivity data, which is of the order of 2%, and the error in the background term, which is also of the order of 2%. The error is about 2% in η and 3% in $(\partial P/\partial T)_{\rho_c}$. Then R_c^* is determined with an uncertainty of the order of 12%. The various quantities which are needed to calculate R_c^* are given in Table XII. [20].

Table XII. Critical Parameters for a Number of Fluids

Substance	T_c (K)	P_c (MPa)	ρ_c ($kg \cdot m^{-3}$)	$(\partial P/\partial T)_{\rho_c}$ ($MPa \cdot K^{-1}$)	Z_c	Y_c	a (10^{-10} m)	$\lambda_B(T_c, \rho_c)$ ($W \cdot m^{-1} \cdot K^{-1}$)
Ar	150.725	4.865	535	0.191	0.289	4.931	7.53	
Xe	289.747	5.840	1110	0.120	0.286	4.953	8.81	
CH_4	190.555	4.595	162.7	0.149	0.285	5.213	8.30	0.0469
C_2H_4	282.344	5.039	214.2	0.118	0.281	5.634	9.17	0.0464
C_2H_6	305.33	4.871	206.5	0.106	0.279	5.663	9.52	0.0437
C_3H_8	369.82	4.247	221	0.080	0.275	6.011	10.63	0.0443
n-C_4H_{10}	425.16	3.800	228	0.064	0.274	6.221	11.56	0.0467
i-C_4H_{10}	407.84	3.629	225.5	0.063	0.275	6.100	11.57	0.0436
n-C_5H_{12}	469.65	3.364	237	0.054	0.262	6.539	12.44	0.0472
CO_2	304.107	7.372	467.7	0.173	0.274	6.016	8.28	0.0363
H_2O	647.067	22.046	322.78	0.275	0.228	7.086	7.40	0.214
D_2O	643.89	21.671	356.24	0.260	0.227	6.725	7.43	0.192
NH_3	405.4	11.303	235	0.207	0.243	6.453	7.91	0.126
SF_6	318.687	3.760	737	0.084	0.281	6.118	10.53	0.0346

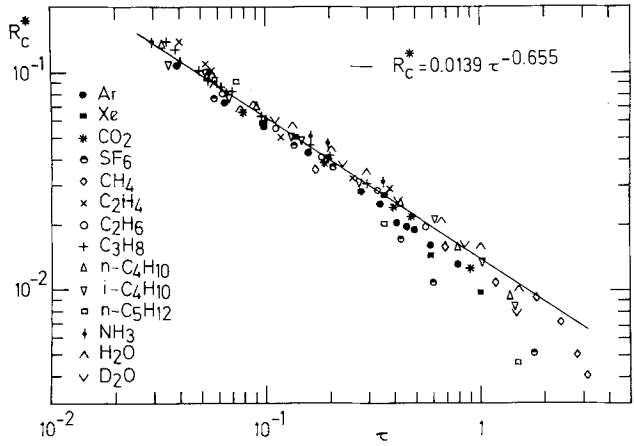

Fig. 1. Variation of R_c^* in terms of the scaled temperature difference $\tau = Y_c(T - T_c)/T_c$.

In the scaled reduced-temperature range $0.03 < \tau < 3$, R_c^* can be represented by the power law

$$R_c^* = R\tau^{\varphi} = 0.0139\tau^{-0.655} \tag{10}$$

where the quantities $R = 0.0139$ and $\varphi = -0.655$ are, respectively, the effective values of the amplitude and the critical exponent. The standard deviation of Eq. (10) is 14.7%. Inversely, if we assume that R_c^* is a unique function of τ, the critical enhancement of the thermal conductivity can be calculated for any fluid. Along the critical isochore an equation, having a similar form as Eq. (10), was previously reported in the literature as

$$\Delta\lambda \sim t^{\varphi} \tag{11}$$

In Eq. (11), the value of the critical exponent φ will also depend on the temperature range which is considered. In an early perturbation theory for the determination of transport coefficients, Kadanoff and Swift [21] found asymptotically $\varphi = -\gamma + \nu$, neglecting the small viscosity divergence. Later Sengers and Keyes [5] introduced the separation between background and anomalous contributions for the thermal conductivity. They found $\varphi = -0.60 \pm 0.05$ for carbon dioxide. Trappeniers [22] found $\varphi = -0.64$ for argon and -0.62 for xenon, but a larger slope far away from T_c. Nieto de Castro and Roder [23] have reported $\varphi = -0.63$ for argon. For pure methane and pure ethane Friend and Roder [24] reported a slightly lower value ($\varphi = -0.56$). In a review paper on transport proper-

ties of fluids near their critical point Sengers [25] suggested that $\varphi = -(1-\tilde{\eta}-z)\nu$, where $\tilde{\eta}=0.03$, $z=0.054$ and $\nu=0.63$, then $\varphi=-0.58$.

The exponent $\varphi=-0.655$, which we have selected in Eq. (10), is larger than the exponents which were proposed in the literature. However, it is easy to show that if we decrease our value of φ, this will not greatly change the standard deviation. On the other hand, a rough estimate of the effective exponent φ_{eff} of Eq. (10) can be made from the effective static behavior. In our experimental temperature range the effective exponent of the isothermal compressibility $\gamma_{\text{eff}}=-1.16$. The effective exponent of the correlation length is difficult to estimate, as there are no experimental data, but it can vary from 0.63 to 0.50. If we consider that $\varphi_{\text{eff}} \simeq -0.66$, this will yield $\nu_{\text{eff}}=0.50$. In fact, we think that along the critical isochore, any effective critical exponent φ_{eff} from -0.57 to -0.66 can be selected.

The corresponding calculated thermal-conductivity enhancement is given in column 3 of Tables I to XI. The deviation between experimental data and calculated data are reported in column 4. However this deviation is not really significant, as a large deviation in $\Delta\lambda_c$, which is small by comparison to λ_B (last column in Table XII), for $\tau \simeq 1.5$, will result in a small deviation for the whole thermal conductivity λ. A better comparison would have been between experimental and calculated thermal-conductivity data, but this is significant only if the effect of density is included in the model.

To test our model, we have also calculated $\Delta\lambda_c$ for some other fluids for which the thermal conductivity was measured in other laboratories with a parallel-plate apparatus and with a transient hot-wire method. The comparison is shown in Table XIII for argon [26], in Table XIV for xenon [27], in Table XV for CH_4 [28], and in Table XVI for CO_2 [29]. The

Table XIII. Thermal-Conductivity Enhancement of Argon Along Its Critical Isochore [26]

T (K)	$\Delta\lambda_c$ exp ($W \cdot m^{-1} \cdot K^{-1}$)	$\Delta\lambda_c$ cal ($W \cdot m^{-1} \cdot K^{-1}$)	Deviation (%)
151.88	0.0377	0.0440	−16.7
152.67	0.0263	0.0312	−18.6
153.71	0.0200	0.0235	−17.5
155.23	0.0158	0.0179	−13.3
159.21	0.0098	0.0117	−19.4
161.02	0.0090	0.0102	−13.3
163.19	0.0075	0.0090	−20.0
164.78	0.0070	0.0083	−18.6
165.71	0.0065	0.0079	−21.6
168.30	0.0054	0.0071	−31.4
174.68	0.0043	0.0057	−32.5

Table XIV. Thermal-Conductivity Enhancement of Xenon Along Its Critical Isochore [27]

T (K)	$\Delta\lambda_c$ exp ($W \cdot m^{-1} \cdot K^{-1}$)	$\Delta\lambda_c$ cal ($W \cdot m^{-1} \cdot K^{-1}$)	Deviation (%)
293.16	0.0215	0.0198	7.9
298.34	0.0119	0.0108	9.2
310.63	0.0062	0.0060	3.2
323.03	0.0033	0.0043	−30.3
347.82	0.0019	0.0028	−47

Table XV. Thermal-Conductivity Enhancement of Methane Along Its Critical Isochore [28]

T (K)	$\Delta\lambda_c$ exp ($W \cdot m^{-1} \cdot K^{-1}$)	$\Delta\lambda_c$ cal ($W \cdot m^{-1} \cdot K^{-1}$)	Deviation (%)
197.9	0.022	0.0267	−21.3
215	0.0099	0.0109	−10.1
235	0.0067	0.0071	−6

Table XVI. Thermal-Conductivity Enhancement of CO_2 Along Its Critical Isochore [29]

T (K)	$\Delta\lambda_c$ exp ($W \cdot m^{-1} \cdot K^{-1}$)	$\Delta\lambda_c$ cal ($W \cdot m^{-1} \cdot K^{-1}$)	Deviation (%)
307.95	0.0468	0.0509	−8.8
313.15	0.0300	0.0288	4.0
323.15	0.0160	0.0174	−8.8
348.15	0.0080	0.0098	−22.5

critical-conductivity enhancements for methane [28] and carbon dioxide [29] were not tabulated with respect to the density, however, from the figures reported in these papers, it was possible to get a rough estimate of the experimental values. The comparison with the data of other sources is only indicative as the critical enhancement is not determined in the same way. For instance, for argon, the thermal-conductivity excess is temperature and pressure dependent. If we compare the experimental and calculated thermal-conductivity enhancements along the critical isochore, the deviation is generally less than 15%, except for methane, where $\Delta\lambda_c$ is small compared to λ and strongly dependent on the determination of λ_B. The data for argon are systematically lower than those given by our model

and are always outside the range of accuracy of our model. For the other compounds the data are within the error bar of our model. It is obvious that the values of the thermal conductivity will depend on the background term, which was selected with an excess thermal conductivity depending, or not, on the temperature.

5. CONCLUSION

We have reported experimental data for the thermal-conductivity enhancements along the critical isochore of C_2H_6, C_2H_4, C_3H_8, n-C_4H_{10}, i-C_4H_{10}, n-C_5H_{12}, CO_2, H_2O, D_2O, NH_3, and SF_6. We have shown that these data can be correlated by a single equation. The calculated critical enhancements of the thermal conductivity of Ar, Xe, CH_4, and CO_2 along the critical isochore were compared to experimental values obtained in other laboratories. Most of the experimental and calculated values agree within the 12% error bar. We believe that the proposed equation can be used to estimate the critical enhancement of any unknown substance along the critical isochore for $5 \times 10^{-3} < t < 0.15$. The advantage of our model is that no adjustable parameter is necessary to carry on this calculation. The quantities which are required are the critical coordinates (T_c, P_c, ρ_c), the slope of the critical isochore and the viscosity along the critical isochore.

The interest of our model over the other models such as $\Delta\lambda(\rho_c, T) = At^{\varphi}$ is that we can estimate $\Delta\lambda_c$ without any experimental thermal-conductivity data in the critical region. In fact, with our model we have no need to estimate the amplitude of the divergence of the thermal conductivity. If our model is used to calculate the critical enhancement of the thermal conductivity, the accuracy of the total thermal conductivity will be much better than 12%, as the background contribution can be estimated with an accuracy generally better than 2%.

REFERENCES

1. B. Le Neindre, Y. Garrabos, and R. Tufeu, *Ber Buns. Ges. Phys. Chem.* **88**:916 (1984).
2. B. Le Neindre, Ph.D. thesis (University of Paris, Paris, 1969).
3. R. Tufeu, Ph.D. thesis (University of Paris, Paris, 1971).
4. P. Bury, Thesis (University of Paris, Paris, 1971).
5. J. V. Sengers and P. H. Keyes, *Phys. Rev. Lett.* **26**:70 (1971).
6. P. Desmarest and R. Tufeu, *Int. J. Thermophys.* **8**:293 (1987).
7. R. Tufeu and B. Le Neindre, *Int. J. Thermophys.* **8**:1 (1987).
8. C. A. Nieto de Castro, R. Tufeu, and B. Le Neindre, *Int. J. Thermophys.* **4**:11 (1983).
9. J. C. Nieuwoudt, B. Le Neindre, R. Tufeu, and J. V. Sengers, *J. Chem. Eng. Data* **32**:1 (1987).
10. B. Le Neindre, R. Tufeu, P. Bury, and J. V. Sengers, *Ber. Buns. Ges. Phys. Chem.* **77**:262 (1973).

11. R. Tufeu and B. Le Neindre, *Int. J. Thermophys.* **8**:283 (1987).
12. R. Tufeu, P. Bury, and B. Le Neindre, *J. Chem. Eng. Data* **31**:246 (1986).
13. R. Tufeu, D. Y. Yvanov, Y. Garrabos, and B. Le Neindre, *Ber. Buns. Ges. Phys. Chem.* **88**:422 (1984).
14. A. Letaief, R. Tufeu, Y. Garrabos, and B. Le Neindre, *J. Chem. Phys.* **84**:921 (1986).
15. G. A. Olchowy and J. V. Sengers, *Phys. Rev. Lett.* **61**:15 (1988).
16. G. A. Olchowy and J. V. Sengers, *Int. J. Thermophys.* **10**:417 (1989).
17. Y. Garrabos, *J. Phys.* **47**:197 (1986).
18. K. Stephan and K. Lucas, *Viscosity of Dense Fluids* (Plenum Press, New York, 1978).
19. B. Le Neindre, *Viscosité*, K 480 (Techniques de l'Ingénieur, Paris, 1988), p. 1.
20. J. V. Sengers and J. M. H. Levelt Sengers, in *Progress in Liquid Physics*, C. A. Croxton, ed. (Wiley, New York, 1978), p. 103.
21. L. P. Kadanoff and J. Swift, *Phys. Rev.* **166**:89 (1968).
22. N. J. Trappeniers, in *Proc. 8th Symp. Thermophys. Prop.*, J. V. Sengers, ed. (ASME, New York, 1982), p. 232.
23. C. A. Nieto de Castro and H. M. Roder, in *Proc. 8th Symp. Thermophys. Prop.*, J. V. Sengers, ed. (ASME, New York, 1982), p. 241.
24. D. G. Friend and H. M. Roder, *Phys. Rev. A* **32**:1941 (1985).
25. J. V. Sengers, *Int. J. Thermophys.* **6**:203 (1985).
26. B. W. Tiesinga, Ph.D. thesis (University of Amsterdam, Amsterdam, 1980).
27. J. van Oosten, Ph.D. thesis (University of Amsterdam, Amsterdam, 1974).
28. H. M. Roder, *Int. J. Thermophys.* **6**:119 (1985).
29. A. Michels, J. V. Sengers, and P. S. van der Gulik, *Physica* **28**:1201 (1962).